Applied Biological Research 28(2): 147-159; (2026)
DOI: 10.48165/abr.2026.28.01.16

THERAPEUTIC POTENTIAL OF *Dipsacus inermis*-DERIVED BIOGENIC ZINC OXIDE NANOPARTICLES: ANTIBACTERBIAL ACTIVITY AND CANCER CELL CYTOTOXICITY

Arfa Ji[1,2], T.A. Sofi[2*], Ehtishamul Haq[1], Ishtiyak Ahmad Peerzada[3], Shahnaz Anjum[4], Saira Banoo[2] and Meraj U Din Dar[5]

[1]*Department of Biotechnology, University of Kashmir, Srinagar - 190 006, Jammu & Kashmir (India)*
[2]*Agri-Nanotechnology Laboratory, Faculty of Horticulture, S.K. University of Agricultural Sciences and Technology of Kashmir (SKUAST-K), Shalimar, Srinagar - 190 025, Jammu & Kashmir (India)*
[3]*Centre of Excellence on Herbal Technology,* [5]*Division of Forest Products & Utilization, Faculty of Forestry, SKUAST-K, Benhama -191 201, Jammu & Kashmir (India)*
[4]*Department of Botany, Lovely Professional University, Phagwara - 144 411, Punjab (India)*
*****e-mail: *sufitariq1@skuastkashmir.ac.in*

(Received 23 December, 2025; accepted 11 March, 2026)

ABSTRACT

Biological synthesis of metallic nanoparticles using plant extracts is a sustainable, low-cost, and eco-friendly alternative to conventional physico-chemical methods. In this study, zinc oxide nanoparticles (ZnONPs) were synthesized for the first time using the aqueous extract of underutilized medicinal herb *Dipsacus inermis*, rich in phytochemicals. The synthesized nanoparticles were thoroughly characterized by UV-vis spectroscopy, dynamic light scattering, scanning electron microscopy, Fourier transform infrared spectroscopy, and X-ray diffraction to confirm nanoscale dimensions, crystalline ZnO structure, and phytochemical-mediated surface functionalization. The characterization studies revealed that the phytochemicals in the extract simultaneously acted as bio-reducing and stabilizing agents and further confirmed the formation of spherical nanoparticles with an average hydrodynamic diameter of 37 nm and a crystalline ZnO structure. The synthesized ZnONPs were then evaluated for antimicrobial and cytotoxicity studies, which revealed that the nanoparticles exhibited significant antibacterial activity against *Staphylococcus aureus* and *Escherichia coli*, with respective inhibition zones reaching 9.1 ± 0.2 and 8.9 ± 0.1 mm at 500 µg mL^{-1}. Anticancer potential was assessed on human breast cancer (MDA-MB231) cells and cytocompatibility on human embryonic kidney (HEK293T) cells, which revealed potential anticancer activity with only 37% ± 1.01 cells viable at the highest test concentration of 100 µg mL^{-1} and showed no significant cytotoxicity to normal cells with more than 70% ± 3.6 cells viable at highest test concentration. These findings highlight the potential of *D. inermis*-mediated ZnONP as ecofriendly therapeutic agents with multifunctional properties, including antibacterial activity, emphasizing further biomedical studies.

Keywords: Antibacterial activity, anticancer activity, cytocompatibility, green synthesis, nanoparticles

INTRODUCTION

Nanomaterials are widely used across various fields, including bioengineering, agriculture, and medicine, due to their outstanding physicochemical properties. In recent decades, increasing scientific focus has been toward the sustainable synthesis of therapeutic metal nanoparticles using

natural resources, such as plants and microbes, with dual objective of reducing the harsh chemical by-products and enhancing the safety profiles of pharmaceutical agents (Arfa Ji *et al.,* 2024). These green synthesis strategies aim to provide a safer alternative to traditional chemical routes, which often rely on hazardous reducing agents (Arfa Ji *et al.,* 2025). Currently, toxic chemicals are being increasingly replaced by the extracts of plants and microbes, which primarily contain various phytochemicals and reductase enzymes necessary for bio-reduction. These extracts from plants and microbes are more ecofriendly, cost-effective, and energy efficient. The phyto-constituents in these extracts function both as reducing and *in situ* capping agents, eliminating the need for additional stabilizing agents during nanoparticle formation. The structural diversity of functional groups in these phytochemicals not only facilitates effective reduction of metal precursors but also reduces nanoparticle aggregation and maintains physicochemical stability through steric hindrance and electrostatic repulsion. Furthermore, they cover nanoparticle surfaces and act as natural binders for diverse biological components, hence they are excellent for biomedical applications (He *et al.,* 2017).

Recent advances in green nanotechnology have demonstrated that plant-mediated synthesis of nanoparticles is an efficient and sustainable alternative to conventional physicochemical methods. Numerous studies have reported the successful synthesis of ZnO nanoparticles (ZnONPs) using plant extracts such as *Cymbopogon citratus*, *Euphorbia hirta,* and *Delonix elata*, which exhibit significant antibacterial and biomedical potential (Abdelbaky *et al.,* 2022; Prakash *et al.,* 2025). Metallic oxide nanoparticles (< 100 nm) have numerous applications due to their unique properties, particularly their high surface-to-volume ratio. Nanoparticles serve as a link between bulk materials and their atomic structures, greatly increasing chemical reactivity and biological activity. Various physicochemical methods are now used to produce different types of nanoparticles. However, these approaches are costly, time-consuming, and environmentally damaging. As a result, there is an urgent need for economical, safe, and environmentally sustainable techniques of nanoparticle production. It is worth noting that using plants to produce nanoparticles offers significant advantages over other biological systems, as plant extracts contain a wide array of bioactive chemicals, such as flavonoids, phenolic compounds, alkaloids, and proteins, which facilitate metal ion reduction (Qi *et al.,* 2017). These biomolecules not only reduce metal ions but also stabilize the nanoparticles and enhance their biological activity, thereby improve their utility in biomedical and antimicrobial applications. Metal oxide nanoparticles are important because of their distinct surface composition and huge surface area.

Different salts of Ag, Au, Zn and Fe are used as precursors to produce plant-derived nanoparticles. Zinc oxide nanoparticles (ZnONPs) have attracted significant interest due to their extraordinary stability, biocompatibility, and intriguing pharmacological properties, including antibacterial and anticancer activities. The plant-derived ZnONPs exhibit strong antimicrobial activity against pathogenic bacteria such as *Escherichia coli* and *Staphylococcus aureus*, primarily by inducing oxidative stress and damaging bacterial cell membranes (Murali *et al.,* 2023). Metal-based nanomaterials target multiple sites in biological systems and reduce drug resistance. With widespread use of antibiotics, the problem of microbial resistance is on rise and is predicted to lead to high mortality rates in near future, if not addressed. Metal oxide nanoparticles are thus regarded as promising antibacterial agents due to their catalytic inhibitory action. Zanet *et al.* (2019) studied the underlying mechanism of action of ZnONPs on *Saccharomyces cerevisiae* and showed that the biological efficacy of nanoparticles depends on both dose and composition. Reactive oxygen species (ROS) are known to be the main mediators of ZnO's bactericidal activity, owing to its strong oxidative properties as a semiconductor with a large band gap (Agarwal *et al.,* 2018). Although numerous studies have explored plant-mediated synthesis of ZnONPs, but these are confined to a limited number of well-known medicinal plants, leaving many ethnomedicinally important species unexplored for nanoparticle production. The genus *Dipsacus* is traditionally known for its medicinal properties and contains diverse phytochemicals like phenolics, flavonoids, and bis-iridoids such as cantleyoside and various triterpenoid saponins that possess strong antioxidant and reducing potential (Alhomaidi *et al*., 2022; Mutukwa *et al*., 2022). These

phytochemicals suggest that the species belonging to this genus may serve as effective bio-resource for green nanoparticle synthesis. The indigenous medicinal plant *Dipsacus inermis* is traditionally used in the Himalayan region for various therapeutic purposes but it has not yet been explored for the green synthesis of ZnONPs. Very limited literature is available on NP synthesis using *D. inermis* (Bhat *et al.,* 2024), hence it represents a novel area for further exploration. Therefore, the present study was aimed to synthesize environmentally acceptable and economically viable biogenic ZnONPs using *D. inermis* extract, characterize the synthesized nanoparticles using various physicochemical techniques, and evaluate their cancer cell toxicity and antibacterial potential against two human pathogenic bacteria. This study may fill the existing research gap by exploring this medicinal plant for nanoparticle synthesis and assess its potential biomedical applications.

MATERIALS AND METHODS

The experimental work was conducted at Agri-Nanotechnology Laboratory, Faculty of Horticulture, SKUAST-Kashmir, India, during the year 2023-2025. The highly pure solvents were supplied by Sigma-Aldrich, USA. Zinc acetate dihydrate (98% purity) was procured from Loba Chemie India. Yeast extract and agar agar media were obtained from HiMedia, India. RPMI-1640 medium (≥ 98 purity), fetal bovine serum (FBS) (≥ 98% purity), trypsin **(**≥ 98% purity**),** L-glutamine (≥ 99% purity), and penicillin-streptomycin (pen-strep) **(**≥ 98% purity) were bought from Gibco/Life Technology.

Bacterial strains and cell lines

Bacterial cultures *viz*. *Escherichia coli* (DH5α) and *Staphylococcus aureus* (ATCC29213) were procured from the Department of Nanotechnology, University of Kashmir, Srinagar, India. *S. aureus* (ATCC 29213) is a well-characterized human pathogenic reference strain that is frequently used in antimicrobial susceptibility testing, whereas *E. coli* (DH5α), derived from *E. coli* K-12 lineage, is a well-known Gram-negative model bacterium frequently used in antibacterial screening studies. MDA-MB231 human breast cancer cells and normal human embryonic kidney cells (HEK293T) were obtained from the National Center for Cell Science (NCCS), Pune, India. Both the cell lines were normally maintained in RPMI media supplemented with 10% FBS 1% L-glutamine and 100 g mL^{-1} pen-step in 5% CO_2 incubated at 37°C.

Collection of plant material and preparation of extract

Dipsacus inermis was collected in September 2023 from Kehmil Forest Division, Keran, Kupwara, J&K (latitude: 34°38′34.35″N; longitude: 74°26′33.16″E). The plant specimen was taxonomically identified by the curator at the Centre for Biodiversity and Taxonomy, University of Kashmir, Srinagar, J&K. A specimen was deposited in the Herbarium of the University of Kashmir vide voucher No. 9079-KASH for future reference. The collected aerial parts of plant were washed, shade-dried, and powdered. For extract preparation, 10 g powdered material was mixed with 100 mL distilled water at 60°C.The extract was filtered through Whatman's filter paper and then stored at 4°C for further use (Khairan and Jalil, 2019).

Qualitative phytochemical analysis

A preliminary phytochemical screening of *D. inermis* extract was conducted to assess the presence of naturally occurring bioactive compounds. The tests included Mayer's test for alkaloids (Marzook *et al.,* 2017), alkaline reagent test for flavonoids (Kancherla *et al.,* 2019), foam test for saponins (Prabhakar and Rao 2024), ferric chloride test for phenols (Sivakumar *et al.,* 2025) and Millon's test for proteins (Godlewska *et al.,* 2022).

Nanoparticle synthesis

For standardizing the optimum synthesis conditions, various experimental parameters *viz*., pH (3-10),

temperature (20-80°C), reaction time (30-120 min), zinc acetate concentration (0.001, 0.01, 0.1, 1.0, and 5 M) were assessed. Different volume ratios of *D. inermis* extract to zinc salt solution (1, 5, 10, 15 and 20 mL) were systematically studied. The pH of reaction mixture was adjusted to test pH level using 0.1 N NaOH or 0.1 N HCl, and the reaction was performed under continuous stirring at room temperature. The formation of ZnONPs was initially indicated by a visible change from light yellow to brownish colour, suggesting the reduction of zinc ions and nucleation of nanoparticles. The synthesized nanoparticles were then collected by centrifugation, washed with distilled water to remove unreacted residues, and dried for further studies (Deepa *et al.,* 2023, Tabasum *et al.,* 2025).

Characterization of nanoparticles

To ensure reproducibility the biogenesis was confirmed by exploring different characteristics of nanoparticles. Dynamic light scattering instrument (Litesizer 500 Anton Paar) at 25°C with a scattering angle of 90° provided information on the hydrodynamic diameter of the synthesized NPs (Mourdikoudis *et al.,* 2018). The nanoparticle suspension was diluted with deionized water to avoid multiple scattering effects. Each sample was measured in triplicates, and the average values were reported. UV-visible spectrophotometry (PerkinElmer Lambda 365) was employed to measure the optical properties of the biosynthesized NPs across 300-600 nm with a 1 cm path length. The scan speed was set at 480 nm min^{-1} with a spectral bandwidth of 1 nm, and deionized water was used as a blank for baseline correction. Scanning electron microscopy (GeminiSEM 500, Carl Zeiss, Germany) was used to determine the size, shape, surface morphology, and aggregation status of NPs, as well as to image the capping of NPs with organic molecules used during green synthesis.
The nanoparticle dispersion was drop-cast onto an aluminium stub, allowed to dry at room temperature, and then coated with gold sputter. High vacuum conditions were used to record the images at an accelerating voltage of 5-15 kV and a working distance of roughly 8-10 mm (Rector *et al.,* 2019). Images were captured at different magnifications to evaluate particle morphology and aggregation patterns. Multiple images were recorded to ensure homogeneity, and particle size was estimated using ImageJ software**.**

The elemental composition and purity of synthesized nano-particles were determined using energy dispersive X-ray spectroscopy (EDX/EDAX) coupled with scanning electron microscopy (Gemini SEM 500, Carl Zeiss, Germany)**.** The analysis was carried out using an EDX detector under an accelerating voltage of 15-20 kV**.** The nanoparticle samples were drop-cast onto aluminium stubs, dried at room temperature, and sputter-coated with a thin gold layer prior to analysis to enhance conductivity. Elemental spectra were recorded from multiple regions of the sample surface to confirm the uniform distribution of elements. The resulting spectra were analysed for qualitative and quantitative elemental composition of the nanoparticles**.**

The presence of functional groups was confirmed by FTIR spectroscopy on Perkin Elmer spectrophotometer. The spectra were recorded in the spectral range of 4000-400 cm^{-1} with a resolution of 4 cm^{-1} and 32 scans per sample. For crystallinity, XRD patterns were recorded using CuK α anode operating at 30.0 mA and 40.0 kV was used in the analysis. The examination was performed at room temperature and samples were scanned at a rate of 2° min^{-1} throughout a 2θ range of 20° to 100° using RIGAKU X ray diffractometer. The diffraction angle (2θ) was found to be a function of the diffracted X-ray intensity (El-Fitiany *et al*., 2024). All measurements were performed in triplicate (n = 3) to ensure the reproducibility of data.

Antimicrobial activity

Green-synthesized ZnONPs and ampicillin (≥ 98% purity) were evaluated for their antibacterial activity against two model pathogenic bacteria, i.e., Gram-positive *Staphylococcus aureus* and Gram-negative *Escherichia coli*. A stock solution of ampicillin was prepared in sterile distilled water and diluted to the required concentrations prior to use. Antimicrobial activity was measured using the disc diffusion method (Abdelbaky *et al.,* 2022) with slight modifications. Yeast extract medium was prepared and autoclaved at 121°C for 30 min. Bacterial cultures were subcultured in flasks containing the autoclaved medium and transferred to a shaking incubator at 37°C for 24 h. of

Fresh culture (250 µL) was loaded on agar plates, and uniform lawns were achieved with sterilized cotton swabs. The 6 mm filter discs loaded with varying concentrations (50, 100, 250, and 500 µg mL^{-1}) of synthesized nanaoparticles and were kept on petri dishes with ampicillin (1mg mL^{-1}) and water was loaded as positive and negative controls, respectively, plant extract (100%), metal salt (1 mg mL^{-1}) served as other controls. The Petri-dishes were incubated at 37°C for 24 h and the zone of inhibition was measured using a sterile ruler (Sivakumar *et al.*, 2025). The experiment was performed in triplicates in a completely randomized design (CRD).

Cytotoxic studies

Human embryonic kidney (HEK293T cells) cells and human breast cancer (MDA-MB231) cells were grown in RPMI-1640 media supplemented with 10% fetal bovine serum and 1% penicillin-streptomycin at 37°C and 5% CO_2. Cytotoxicity of biosynthesized NPs was assessed using 3-(4,5 dimethylthiazol-2-yl) 2,5 diphenyltetrazolium bromide (MTT) assay, which measures metabolic activity and toxicity in living cells. Cells were seeded in 96 well plates and exposed to ZnONPs at different concentrations (12.5, 25, 50, & 100 µg mL^{-1}) for 24 h. After exposure, MTT solution at 5 mg mL^{-1} was added to the cells treated with ZnONPs and the plates incubated for 4-5 h. The formazan crystals produced by the reduction of MTT dye was dissolved using DMSO and absorbance measured at 563 nm using ELISA plate reader (Genetix) (Amin *et al.*, 2024). The experiment was carried out in CRD with each treatment replicated thrice to ensure reproducibility.

Statistical analysis

Each experiment was carried out in triplicate in CRD design. Origin 9.0 (*https://www.originlab.com/*) and ImageJ software (*https://imagej.nih.gov/ij/*) were used to evaluate data from various experiments conducted to characterize the NPs. Furthermore, Prism 7.0 (GraphPad Software Inc., USA) was used to evaluate the antimicrobial and cytotoxicity data. Data were presented as mean ± standard deviation and one-way ANOVA was used to establish statistical significance with $P < 0.0001$ considered statistically significant.

RESULTS AND DISCUSSION

Qualitative phytochemical screening

The phytochemical screening of the plant extract confirmed the presence of alkaloids, flavonoids, phenols and proteins, which play a crucial role in NP synthesis as reducing and stabilizing agents. The absence of saponins suggests the involvement of other bioactive compounds in ZnONP formation, as also reported by Abdelbaky *et al.* (2022). Plant extract functions as stabilizing and capping agent during NP synthesis. Multiple hydroxyl and carbonyl functional groups facilitate metal ion reduction and simultaneously prevent NP agglomeration through surface adsorption and steric stabilization.

Optimization of synthesis parameters for ZnONPs

The formation of ZnONPs was initially indicated by a visible change in colour of reaction mixture, confirming the reduction of zinc ions mediated by phytochemicals present in *Dipsacus inermis* extract. Different synthesis parameters *viz*., pH, temperature, reaction time, zinc salt concentration, plant extract volume, were investigated to determine the optimum conditions for nanoparticle formation. It was observed that increasing the plant extract volume from 5 to 20 mL enhanced nanoparticle formation due to the higher availability of phytochemicals acting as reducing and stabilizing agents. A complete reduction of Zn+ with good colour intensity was obtained at 10:1 volume ratio of zinc salt solution to plant extract. The temperature was varied from 20 to 80°C and it was observed that the colour becomes darker with rising temperature. As the temperature approached around 60° the colour became more dark suggesting an increase in NP yield. Similarly, a moderate concentration of zinc acetate (0.1 M) was found suitable for stable nanoparticle formation, whereas lower concentration (0.001 M) resulted in slower reaction and higher

concentration (5 M) promoted aggregation. The reaction time of 60 min was found sufficient for efficient nucleation and growth of nanoparticles. Furthermore, alkaline pH conditions favoured ZnONP formation compared to the acidic conditions which was indicated by observing darker colour at pH 8. At high basic conditions, the intensity of colour was low indicating that slight alkaline pH was best condition for the formation of ZnONPs (Tabasum *et al.*, 2025).

Particle size and zeta potential analysis of synthesized NPs

Dynamic light scattering (DLS) analysis confirmed that ZnONPs were uniformly dispersed in aqueous medium, with an average hydrodynamic size of 37.61 nm (Fig. 1a) and a polydispersity index of 27.41%. The presence of a single, sharp peak with 100% intensity in size distribution profile indicated high monodispersity and the absence of seemingly large aggregates and/or poly-disperse particles. The nanoscale dimension obtained were consistent with the expected particle size for ZnO in various applications, thereby enhancing its surface reactivity and size-dependent properties, such as optical absorption and antimicrobial activity (Abdelbaky *et al*., 2022). This study also discusses the importance of the polydispersity index and the connection between DLS and the actual particle core size. Since DLS measures the hydrodynamic size, which includes the particle core and any solvation layer, the actual physical core size may be slightly smaller. Nevertheless, the single-peak distribution strongly supported the successful synthesis of stable and uniform ZnONPs suitable for further functional studies. Similar results have earlier been reported (Chakra *et al*., 2025).

Zeta potential analysis was performed to detect the surface charge of synthesized ZnONPs. The mean zeta potential value of synthesized ZnONPs was -7.55 mV (Fig. 1b). The results confirmed that

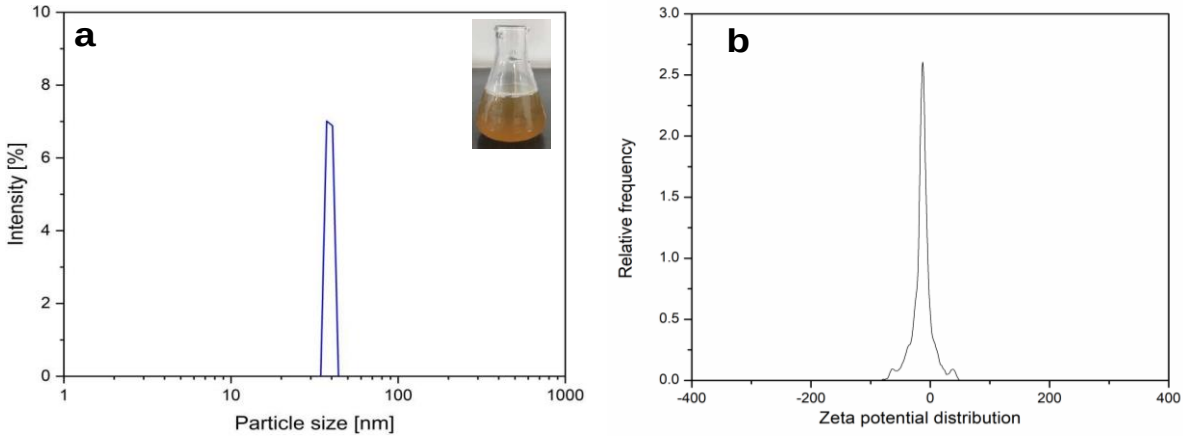

Fig. 1: (a) Average hydrodynamic size, (b) Zeta potential of the synthesized ZnONPs

the capping biomolecules present on ZnONPs were mostly of negatively charged groups. The negative charge detected on ZnONPs indicated electrostatic repulsion between the synthesized NPs.

UV-vis spectroscopy

The UV-visible spectra of *D. inerims* extract and ZnONPs were obtained from 300 to 600 nm. ZnONPs generally exhibit strong UV absorption due to their wide band gap and distinctive surface characteristics. ZnONPs synthesized using *D. inerims* aqueous extract exhibited surface plasmon resonance at 373 nm, which confirms the successful synthesis of ZnONPs (Fig. 2). These SPR peaks reportedly arise from the collective electron oscillations at the NP's surface, which depend on

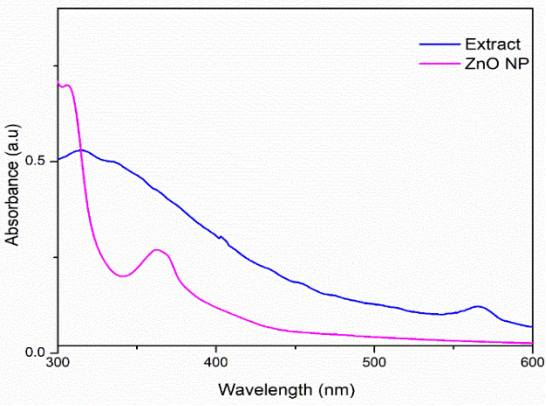

Fig. 2: UV-visible spectrum showing the absorption peak of *Dipsacus inerims* extract and ZnONPs

size, shape, and the surrounding environment. Although conventional ZnONPs usually absorb at slightly higher wavelengths, the observed shift may be due to smaller size and interactions with phytochemicals from *D. inermis* (Mohammadian *et al*., 2018). Since no other peaks were seen in the spectrum, its supports the conclusion that only ZnONPs were synthesized (Maher *et al.*, 2023).

SEM analysis

Based on the SEM analysis, ZnONPs were spherical in shape, with some degree of agglomeration observed at both 100 and 500 nm scales (Fig. 3a-b). The average size was 45.80 nm (Fig. 3c). This level of aggregation is expected due to NP drying. Such agglomeration and variable sizing are consistent with previously reports, wherein SEM images revealed that ZnONPs often appear as spongy, spherical clusters with variable aggregation depending on synthesis conditions and differences in stabilizing agents (Jayappa *et al.*, 2020; Shashanka *et al.*, 2020).

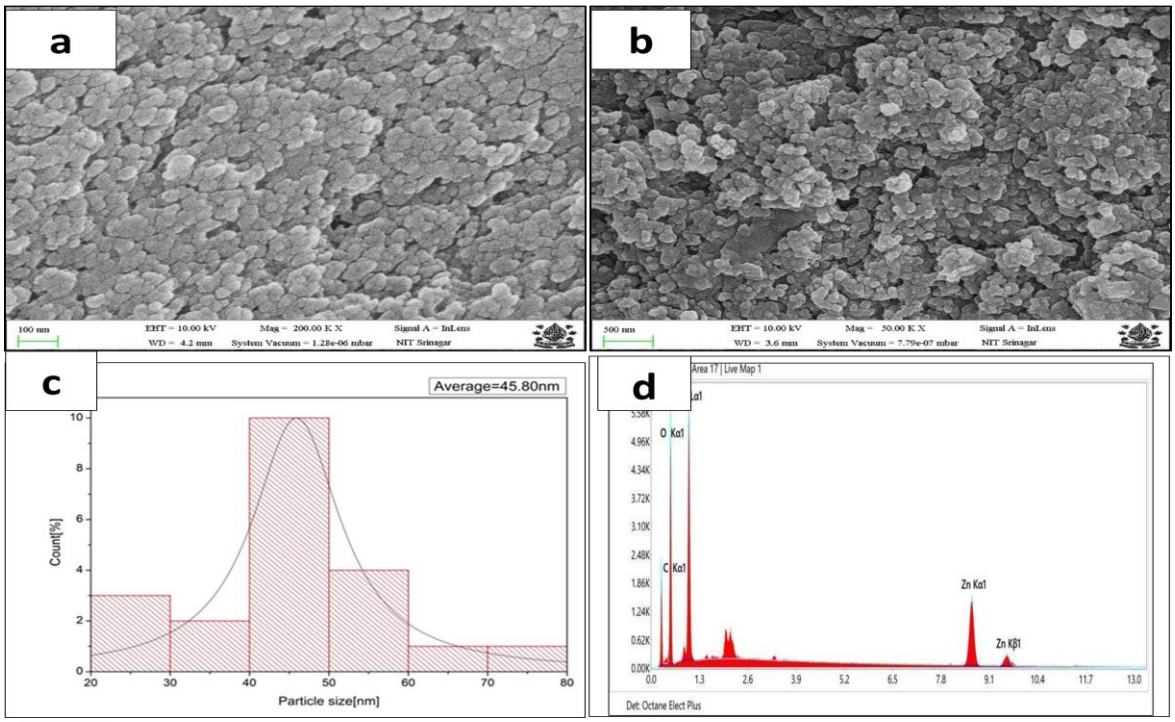

Fig. 3: SEM images of ZnONPs at different scales; a) high-magnification image (200K) with a scale bar of 100 nm; b) low-magnification image taken at 50K with a scale bar of 500 nm; c) Histogram depicting the average size; (d) EDX spectrum of synthesized ZnONPs

Energy-dispersive X-ray (EDX) analysis was performed to determine the elemental composition of synthesized ZnONPs. The spectrum exhibited characteristic peaks corresponding to Zn and O**,** confirming the formation of ZnONPs (Fig. 3d). The quantitative analysis indicated an atomic percentage of 6.9% for Zn and 35.9% for O. The relatively lower Zn signal may be attributed to the presence of organic phytochemical residues originating from the plant extract used during green synthesis, which act as reducing and stabilizing agents and contribute significantly to the surface composition detected by EDX. Additionally, the use of carbon tape and the surface-sensitive nature of EDX analysis may enhance the contribution of light elements thereby reducing the relative Zn percentage. Similar observations have been reported on plant-mediated synthesis of ZnONPs where organic capping layers influence the elemental composition detected by EDX (Jayachandran *et al.*, 2021; Sarwar *et al.*, 2025; Anjum *et al.*,2025). Nevertheless, the presence of distinct Zn and O peaks supports the successful formation of ZnO nanoparticles. Table 1 shows the quantitative EDX elemental weight% and atomic%.

Table 1: Quantitative EDX elemental table

Element	Weight (%)	Atomic (%)
C K	40.1	57.2
O K	33.6	35.9
Zn K	26.3	6.9

XRD analysis

The peaks in XRD analysis confirmed the crystallinity of the synthesized NPs, as evidenced by the distinct diffraction peaks observed in the 2θ range of 20° to 80°. The full width at half maximum (FWHM) value of the graph is 0.020131 radians. The specific peaks at 21.28°, 22.46°, 29.30°, 31.70°, 33.27°, 37.00°, 47.30°, 59.34°, and 69.76° correspond to crystallographic planes were indicative of ZnO's characteristic Wurtzite hexagonal structure (Fig. 4), consistent with the standard JCPDS card No. 36-1451 (Faisal *et al*., 2021). Additional peaks may be attributed to the presence of organic phytochemical residues from the plant extract used during green synthesis**,** which act as reducing and stabilizing agents for nanoparticle formation. Similar additional reflections have been reported in plant-mediated synthesis of ZnONPs. The broadening of these diffraction peaks is primarily attributed to the nano-scale particle size, which induces broadening due to the finite crystallite-size effect, as described by the Debye–Scherrer equation. Smaller crystallite sizes correlate with broader peaks, a common phenomenon in XRD analysis (Nigam and Pawar, 2020).

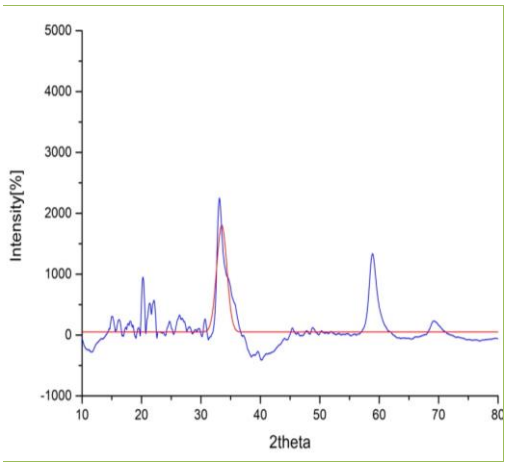

Fig. 4: XRD pattern of ZnONPs showing the characteristic peaks confirming the hexagonal Wurtzite crystalline structure

FTIR analysis of synthesized ZnONPs

The FTIR spectra of the synthesized ZnONPs displayed distict peaks at 645 and 510 cm^{-1} (Fig. 5), which are indicative of Zn-O stretching vibrations, thereby verifying the synthesis of ZnONPs with metal-oxygen bonding (Zn-O). Other peaks in the spectra corresponded to various functional groups, most likely originating from leftover organic molecules or surface-adsorbed species. The presence of these functional groups indicates that surface capping and/or stabilizing agents may be present in trace amounts, possibly derived from synthesis precursors or solvents, and play a role in controlling particle growth and preventing agglomeration during ZnONP formation (Yuan *et al.*, 2021; El-Faroudi *et al.*, 2023). Broad bands observed at 3779 and 3653 cm^{-1} correspond to O–H stretching vibrations of phenolic and alcoholic groups, while the peak at 2949 cm^{-1} is attributed to C–H stretching vibrations of aliphatic compounds. The band near 1479 cm^{-1} indicates aromatic C=C stretching, and peaks around 1302 and 1173 cm^{-1} correspond to C–N and C–O stretching vibrations, respectively. These functional groups likely originate from plant metabolites and play a vital role in the reduction and stabilization of nanoparticles during green synthesis. Importantly, the characteristic absorption bands observed at 645 and 510 cm^{-1} correspond to Zn–O stretching vibrations**,** confirming the formation of ZnONPs. The presence of organic functional groups indicates the adsorption of phytochemical residues on the nanoparticle surface, which act as natural capping and stabilizing agents. Phenols and flavonoids are considered the main contributors among these phytochemicals because of their potent reducing capabilities, which allow the

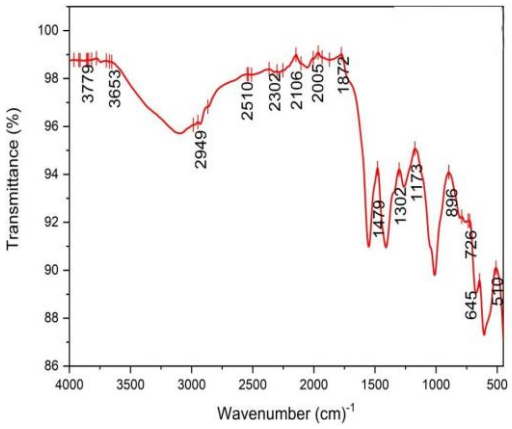

Fig. 5: FTIR spectrum showing functional groups from phytochemicals and characteristic Zn–O stretching vibrations (400-600 cm^{-1}) confirming ZnO nanoparticles

conversion of Zn^{2+} ions to ZnONPs by providing electrons during the reduction process (Iravani, 2011; Ahmed *et al.*, 2016). Furthermore, proteins and alkaloids can work as capping or stabilizing agents by attaching to the surface of nanoparticles via functional groups like –OH, –NH, and C=O. This prevents aggregation and improves nanoparticle stability. The presence of these functional groups was further confirmed by FTIR analysis, which revealed characteristic absorption bands for hydroxyl, amine, and carbonyl groups. Interestingly, saponins were not detected in the phytochemical screening, implying that other bioactive chemicals, particularly phenolic and flavonoid contents, are primarily responsible for the reduction and stabilizing processes involved in ZnONP synthesis. Similar methods have been frequently described in plant-mediated nanoparticle formation, with polyphenolic chemicals acting as both reducing and stabilizing agents (Jayachandran *et al.*, 2021). As a result, the phytochemicals in *D. inermis* extract are expected to have a dual role in ZnONP production and surface functionalization.

Antibacterial effect of synthesized NPs.

ZnONPs have concentration-dependent antibacterial activity against *E. coli* and *S. aureus* (Fig. 6). The zones of inhibition gradually increased with increasing NP concentration, reaching 3.1 ± 0.2 to 9.1 ± 0.2, and 2.9 ± 0.3 to 8.9 ± 0.1 mm from 50 to 500 µg mL^{-1} in *E. coli* and *S. aureus*, respectively. Both bacterial strains have comparable susceptibility patterns, with *E. coli* showing slightly higher sensitivity than *S. aureus* across all the concentrations. The positive control exhibits the widest zone of inhibition, supporting the experimental protocol's validity and reproducibility. ZnONPs demonstrated broad-spectrum antibacterial activity via different mechanisms. Their positively charged surface charge facilitates robust interactions with negatively charged bacterial cell walls, resulting in membrane rupture. The generation of reactive oxygen species (ROS) can cause oxidative stress, damage bacterial DNA, proteins, and lipids and, as a result, jeopardize the cell integrity and viability. Additionally, the emission of Zn^{+} ions can disrupt microbial metabolism, inhibiting growth significantly. Statistically significant results ($P \leq 0.0001$) highlight the reproducibility and efficacy of ZnONPs as antimicrobial agents (Kim *et al.*, 2020).

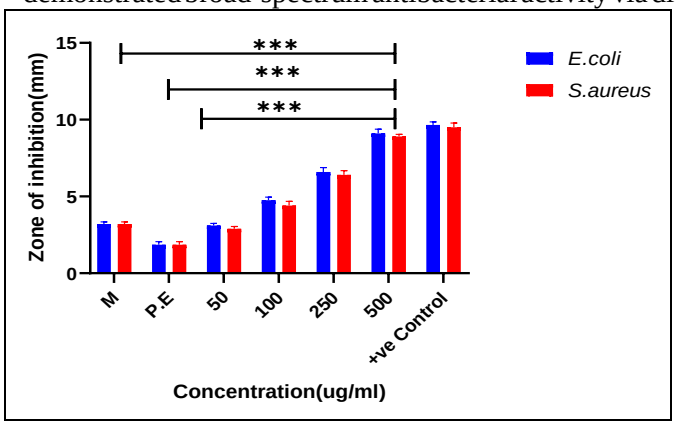

Fig. 6: Concentration-dependent antibacterial activity of ZnONPs against *E. coli* and *S. aureus* (P<0.0001)

Cytotoxicity studies

ZnONPs significantly decreased the viability of MDA-MB231 breast cancer cells in a dose dependent manner, as demonstrated in (Fig. 7A). Only about 37% ±1.01 of the cancer cells remained viable at the highest tested concentration of 100 µg mL^{-1}, indicating a marked decrease in

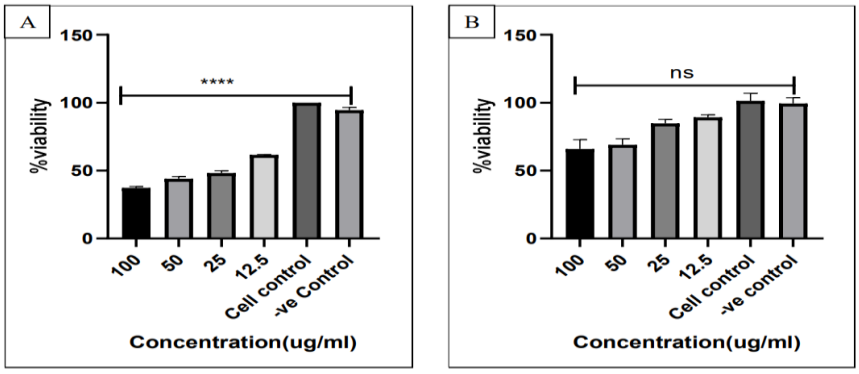

Fig. 7: Dose-dependent effect of ZnONPs on the viability of A) breast cancer (MDA-MB231) cells, B) human embryonic kidney (HEK293T) cells (P < 0.0001).

cancer viability and significant potential of the synthesized NPs in anticancer applications. In contrast, the viability of normal cells was significantly preserved at the same tested concentrations, with over 70% ± 3.6 cells viable at the highest tested concentration (Fig. 7B). This selectivity is important for potential clinical applications because it minimizes damage to healthy cells. These findings are in line with a previous study that demonstrates how ZnONPs cause cytotoxicity in cancer cells by inducing apoptosis, depolarizing the mitochondrial membrane, and increasing ROS production. Normal cells, on the other hand, are less damaged because of a more robust antioxidant defense system (Yuan *et al.*, 2021).

Conclusion: The current study illustrates the green synthesis of ZnONPs using an aqueous extract of *Dipsacus inermis*, leveraging the plant's rich phytochemical profile to simultaneously facilitate NP formation and stability. Comprehensive characterization verified the nanoscale size, crystallinity, and purity of the synthesized ZnONPs. The NPs exhibited potent antibacterial effects against clinically relevant pathogens This biosynthetic approach offers an eco-friendly, economically viable alternative to conventional chemical synthesis methods, so as to minimize the environmental impact and reduce toxic waste. The observed selective toxicity suggests the potential for further development of ZnONPs in targeted cancer therapies. Future studies must explore on *in vivo* efficacy, elucidate detailed mechanistic pathways, and develop large-scale production methods to advance their biomedical applications.

Acknowledgments: The authors sincerely acknowledge the support of the Division of Plant Pathology and Agri-Nanotechnology Laboratory, SKUAST-Kashmir, Shalimar, Srinagar (J&K) and the University of Kashmir, Srinagar (J&K) for making this research work possible. We also acknowledge the Central Research Facility Center, National Institute of Technology, Srinagar, J&K, India, for assistance with respect to the facilities for UV-vis, PSA, SEM, EDX, XRD, and FTIR analysis. We acknowledge Akhter H. Malik, Curator of the KASH Herbarium at the Center for Biodiversity and Taxonomy, University of Kashmir, for help in the proper identification of plant specimen.

Author's contribution: Arfa Ji: Executed the experimental plan, employed softwares and prepared the original draft; T.A. Sofi: Conceptualization, resource management, supervision and fund acquisition; Ehtishamul Haq: Supervision, reviewed manuscript; I.A. Peerzada: Reviewed the manuscript and analysed the data; Shehnaz Anjum: Formal data analysis; Saira Banoo: Reviewed the work and draft preparation; and Meraj U Din Dar: performed statistical analysis of data and final draft preparation.

Funding: The authors received no funding for this work.

Conflict of interest: The authors declare that they have no conflict of interest regarding the work presented in the manuscript.

REFERENCES

Abdelbaky, A.S., Abd El-Mageed, T.A., Babalghith, A.O., Selim, S. and Mohamed, A.M. 2022. Green synthesis and characterization of ZnO nanoparticles using *Pelargonium odoratissimum* (L.) aqueous leaf extract and their antioxidant, antibacterial and anti-inflammatory activities. *Antioxidants*, **11**: 1444. [*https://doi.org/10.3390/antiox11081444*].

Agarwal, H., Menon, S., Kumar, S.V. and Rajeshkumar, S. 2018. Mechanistic study on antibacterial action of zinc oxide nanoparticles synthesized using green route. *Chemico-Biological Interactions*, **286**: 60-70.

Ahmed, S., Ahmad, M., Swami, B.L. and Ikram, S. 2016. A review on plants extract mediated synthesis of silver nanoparticles for antimicrobial applications: A green expertise. *Journal of Advanced Research*, **7**: 17-28.

Alhomaidi, A., Alghamdi, R., Al-Zahrani, M. and Alharbi, A. 2022. Biosynthesis and characterization of silver nanoparticles using medicinal plant extracts and their biological activities. *Green Chemistry Letters and Reviews*, **15**: 529-541.

Al-Marzook, A.H. and Omran, A.H. 2017. Cytotoxic activity of alkaloid extracts of some plants. *Asian Journal of Pharmaceutical and Clinical Research*, **10**: 168-171.

Amin, A., Arfa Ji, Bhat, B.A., Murtaza, D., Hurrah, A.A., Bhat, I.A. *et al.*, 2024. Anti-lung cancer activity of synthesized substituted 1, 4-benzothiazines: an insight from molecular docking and experimental studies. *Anti-Cancer Agents in Medicinal Chemistry-Anti-Cancer Agents*, **5**: 358-371.

Anjum, S., Sofi, T.A., Vyas, A. and Arfa Ji. 2025. Mycogenic production of magnesium nanoparticles for antifungal activity against alternariamali infecting apple (*Malus x domestica*). *Applied Biological Research*, **27**: 137-146.

Arfa Ji, Hamid, A., Andrabi, S.A.H., Ehtishamul Haq, and Tombuloglu, H. 2024. Interaction of nanoparticles with biomolecules. pp. 143-157. **In**: *Molecular Impacts of Nanoparticles on Plants and Algae* (eds. H. Tombuloglt, G. Tombuloglu, G., E. Al-Suhaimi, A. Baykal and K.R. Hakeem). Academic Press, Amsterdam, the Netherlands.

Arfa Ji, Hamid, A., Ehtishamul Haq, Murtaza, D., Amin, A., Hakak, A., *et al.*, 2025. Drug discovery and secondary metabolites - An overview. pp. 1-14. **In**: *Secondary Metabolites and Drug Discovery*. (eds. U.A. Dar, M. Shahnawaz and N. Singh). Wiley Online Library. [*DOI:10.1002/9781394204595*].

Bhatt, K., Agrawal, S., Pattanayak, S.K., Jain, V.K. and Khan, F. 2024. Biofabrication of zinc oxide nanoparticles by using *Lawsonia inermis* L. seed extract. *Inorganic and Nano-Metal Chemistry*, **54**: 1171-1178.

Chakra, P.S., Banakar, A., Puranik, S.N., Kaveeshwar, V., Ravikumar, C.R. and Gayathri, D. 2025. Characterization of ZnO nanoparticles synthesized using probiotic *Lactiplantibacillus plantarum* GP258. *Beilstein Journal of Nanotechnology*, **16**: 78-89.

Deepa, Dhanker, R., Kumar, R., Kamble, S.S., Kamakshi and Goyal, S. 2023. Biosynthesis and characterization of silver nanoparticles generated from peels of *Solanum tuberosum* (potato) and their antibacterial and wastewater treatment potential. *Frontiers in Nanotechnology*, **5**: 1213160. [*https://doi.org/10.3389/fnano.2023.1213160*].

El-Faroudi, L., Saadi, L., Barakat, A., Mansori, M., Abdelouahdi, K. and Solhy, A. 2023. Facile and sustainable synthesis of ZnO nanoparticles: Effect of gelling agents on ZnO shapes and their photocatalytic performance. *ACS Omega*, **8**: 24952-24963.

El-Fitiany, R.A., AlBlooshi, A., Samadi, A. and Khasawneh, M.A. 2024. Biogenic synthesis and physicochemical characterization of metal nanoparticles based on *Calotropis procera* as promising sustainable materials against skin cancer. *Scientific Reports*, **14**: 25154. [*https://doi.org/10.1038/s41598-024-76422-w*].

Faisal, S., Jan, H., Shah, S.A., Shah, S., Khan, A., Akbar, M.T. and Syed, S. 2021. Green synthesis of zinc oxide (ZnO) nanoparticles using aqueous fruit extracts of *Myristica fragrans*: Their characterizations and biological and environmental applications. *ACS Omega*, **6**: 9709-9722.

Gates-Rector, S. and Blanton, T. 2019. The powder diffraction file: A quality materials characterization database. *Powder Diffraction*, **34**: 352-360.

Godlewska, K., Pacyga, P., Szumny, A., Szymczycha-Madeja, A., Wełna, M. and Michalak, I. 2022. Methods for rapid screening of biologically active compounds present in plant-based extracts. *Molecules*, **27**: 7094 [*https://doi.org/10.3390/molecules27207094*].

He, Y., Wei, F., Ma, Z., Zhang, H., Yang, Q., Yao, B. *et al.*, 2017. Green synthesis of silver nanoparticles using seed extract of *Alpinia katsumadai*, and their antioxidant, cytotoxicity, and antibacterial activities. *Royal Society of Chemistry Advances*, **7**: 39842-39851.

Iravani, S. 2011. Green synthesis of metal nanoparticles using plants. *Green Chemistry*, **13**: 2638-2650.

Jayachandran, A., Aswathy, T.R. and Nair, A.S. 2021. Green synthesis and characterization of zinc oxide nanoparticles using *Cayratia pedata* leaf extract. *Biochemistry and Biophysics Reports*, **26**: 100995. [*https://doi.org/10.1016/j.bbrep.2021.100995*].

Jayappa, M.D., Ramaiah, C.K., Kumar, M.A.P., Suresh, D., Prabhu, A., Devasya, R.P., *et al.*, 2020. Green synthesis of zinc oxide nanoparticles from the leaf, stem and *in vitro* grown callus of *Mussa endafrondosa* L.: Characterization and their applications. *Applied Nanoscience*, **10**: 3057-3074.

Kancherla, N., Dhakshinamoothi, A., Chitra, K. and Komaram, R.B. 2019. Preliminary analysis of phytoconstituents and evaluation of anthelminthic property of *Cayratia auriculata* (*in vitro*). *Maedica*, **14**: 350. [*https://doi.org/10.26574/maedica.2019.14.4.350*].

Khairan, K. and Jalil, Z. 2019. Green synthesis of sulphur nanoparticles using aqueous garlic extract (*Allium sativum*). *Rasayan Journal of Chemistry*, **12**: 50. [*https://doi.org/10.31788/RJC.2019.1214073*].

Kim, I., Viswanathan, K., Kasi, G., Sadeghi, K., Thanakkasaranee, S., and Seo, J. 2020. Preparation and characterization of positively surface charged zinc oxide nanoparticles against bacterial pathogens. *Microbial Pathogenesis*, **149**: 104290. [*https://doi.org/10.1016/j.micpath.2020.104290*].

Maher, S., Nisar, S., Aslam, S.M., Saleem, F., Behlil, F., Imran, M., *et al.*, 2023. Synthesis and characterization of ZnO nanoparticles derived from biomass (*Sisymbrium irio*) and assessment of potential anticancer activity. *ACS Omega*, **8**: 15920-15931.

Mohammadian, M., Es'haghi, Z. and Hooshmand, S. 2018. Green and chemical synthesis of zinc oxide nanoparticles and size evaluation by UV–vis spectroscopy. *Journal of Nanomedicine Research*, **7**: 00175. [*https://doi.org/10.15406/jnmr.2018.07.00175*].

Mourdikoudis, S., Pallares, R.M. and Thanh, N.T. 2018. Characterization techniques for nanoparticles: Comparison and complementarity upon studying nanoparticle properties. *Nanoscale*, **10**: 12871-12934.

Murali, M., Gowtham, H.G., Shilpa, N., Singh, S.B., Aiyaz, M., Sayyed, R.Z., *et al.*, 2023. Zinc oxide nanoparticles prepared through microbial mediated synthesis for therapeutic applications: A possible alternative for plants. *Frontiers in Microbiology*, **14**: 1227951. [*https://doi.org/10.3389/fmicb.2023.1227951*].

Nigam, A. and Pawar, S.J. 2020. Synthesis and characterization of ZnO nanoparticles to optimize drug loading and release profile for drug delivery applications. *Materials Today Proceedings*, **26**: 2625-2628.

Prabhakar, Y. and Rao, S. 2024. Phytochemical profiling, green synthesis, and bioactivity evaluation of silver nanoparticles (AgNPs) synthesized from *Ipomoea laxiflora* extract. *Plant Science Archieves*, **9**: 19-30.

Prakash, R., Saravanan, P., Kumar, P., Omer, S.N., and Rajeshkannan, R. 2025. Synergistic green synthesis of ZnO nanoparticles using *Cymbopogon citratus* and *Nelumbo nucifera* for enhanced antibacterial activity. *Sustainable Chemistry One World*, **8**: 100144. [*https://doi.org/10.1016/j.scowo.2025.100144*].

Qi, K., Cheng, B., Yu, J. and Ho, W. 2017. Review on the improvement of the photocatalytic and antibacterial activities of ZnO. *Journal of Alloys and Compounds*, **727**: 792-820.

Sarwar, K., Nazli, Z.I.H., Munir, H., Aslam, M. and Khalofah, A. 2025. Biosynthesis of zinc oxide nanoparticles using *Moringa oleifera* leaf extract, probing antibacterial and antioxidant activities. *Scientific Reports*, **15**: 20413. [*https://doi.org/10.1038/s41598-025-08839-w*].

Shashanka, R., Esgin, H., Yilmaz, V.M. and Caglar, Y. 2020. Fabrication and characterization of green synthesized ZnO nanoparticle based dye-sensitized solar cells. *Journal of Science: Advanced Materials and Devices*, **5**: 185-191.

Sivakumar, S., Rangaswamy, B., Shanmugam, L. and Marudhachalam, K. 2025. Phytochemical mediated zinc oxide nanoparticles from *Euphorbia antiquorum*: Synthesis, characterization and antibacterial activity. *Next Nanotechnology*, **8**: 100210. [*https://doi.org/10.1016/j.nxnano.2025.100210*].

Tabasum, H., Mushtaq, M., Sofi, T.A., Paul, J.A., Bhat, B.A., Malik, A.H., *et al.*, 2025. *Fritillaria cirrhosa* derived biosilver nanoparticles based nanobiopesticide: An effective antifungal agent against cobweb disease in mushroom crop. *Applied Nanoscience*, **15**: 29. [*https://doi.org/10.1007/s13204-025-03109-7*].

Yuan, G., Guan, Y., Yi, H., Lai, S., Sun, Y. and Cao, S. 2021. Antibacterial activity and mechanism of plant flavonoids to gram-positive bacteria predicted from their lipophilicities. *Scientific Reports*, **11**: 10471. [*https://doi.org/10.1038/s41598-021-90035-7*].

Zanet, V., Vidic, J., Auger, S., Vizzini, P., Lippe, G., Iacumin, L., *et al.*, 2019. Activity evaluation of pure and doped zinc oxide nanoparticles against bacterial pathogens and *Saccharomyces cerevisiae*. *Journal of Applied Microbiology*, **127**: 1391-1402.